

# Rho Resonance Parameters from Lattice QCD

Dehua Guo, Andrei Alexandru, Raquel Molina and Michael Döring

Jefferson Lab Seminar

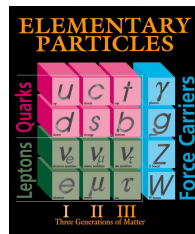
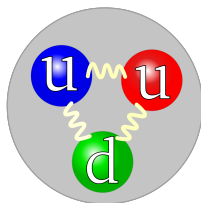
Oct 03, 2016

# Overview

- 1 Introduction to Lattice QCD
- 2 Method
- 3 Results
- 4 Conclusion

# Introduction to Lattice QCD

- Most visible matter in the universe are made up of particles called hadrons.



- The interaction between hadrons is dominated by the strong force.
- Quantum Chromodynamics (QCD) is a theory to describe the strong interaction between quarks and gluons which make up hadrons.

$$\mathcal{L}_{QCD} = -\frac{1}{2} \text{Tr} F_{\mu\nu} F^{\mu\nu} - \sum_f \bar{\psi}_f \gamma^\mu [\partial_\mu - igA_\mu] \psi_f - \sum_f m_f \bar{\psi}_f \psi_f, \quad (1)$$

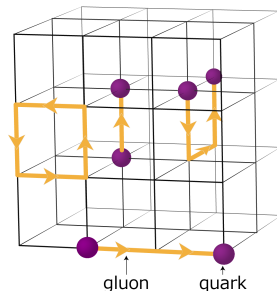
- Some techniques to work with QCD: Perturbation theory, Effective field theory, Lattice QCD and so on.

# Introduction to Lattice QCD

For light hadron study, non-perturbative approach is needed. Lattice QCD is a non-perturbative approach to QCD. It formulates QCD in a discrete way.

Inputs:

- lattice geometry  $N$
- lattice spacing  $a$  set indirectly through the coupling constant  $g$
- quark mass represented by pion mass  $m_\pi$



For light hadron study, only light quarks  $u$  and  $d$  are important.  $s$  quark introduces only small correction.

The role of Lattice QCD in resonance study is to extract the energy spectrum for two hadron states.

# Introduction to Lattice QCD

Why we study resonances from Lattice QCD?

- Lattice QCD offers us a way to study the resonances in terms of quark and gluon dynamics. It serves as a test of QCD for well determined resonance parameters.
- The techniques can be used to investigate systems where the experimental situation is less clear.
- Validate effective models used to describe hadron scattering.

How?

- We start from meson resonance because they have better signal-to-noise ratio.
- $\rho(770)$  resonance in  $I = 1, J = 1$   $\pi$ - $\pi$  scattering channel.

## Symmetries on the lattice

On the lattice, the energy eigenstates  $|n\rangle$  of the system are computed in a given irrep of the lattice symmetry group.

$$\psi_n(R^{-1}x) = \psi_n(R^{-1}(x + \mathbf{n}L)); \quad \langle \hat{O}_2(t) \hat{O}_1^\dagger(0) \rangle = \sum_n \langle 0 | \hat{O}_2 | n \rangle \langle n | \hat{O}_1 | 0 \rangle e^{-tE_n} \quad (2)$$

Isospin, color and flavor symmetries are similar to the continuum.

**Table:** Irreducible representation in  $SO(3)$ ,  $O$  and  $D_4$

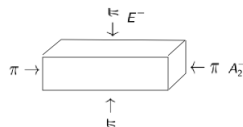
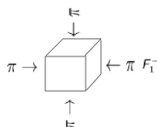
	$SO(3)$	cubic box( $O_h$ )	elongated box( $D_{4h}$ )
irep label	$Y_{lm}; l = 0, 1, \dots, \infty$	$A_1, A_2, E, F_1, F_2$	$A_1, A_2, E, B_1, B_2$
dim	$1, 3, \dots, 2l + 1, \dots, \infty$	$1, 1, 2, 3, 3$	$1, 1, 2, 2, 2$

**Table:** Angular momentum mixing among the irreducible representations of the lattice group

$O_h$		$D_{4h}$	
irreducible representation	$l$	irreducible representation	$l$
$A_1$	0, 4, 6, ...	$A_1$	0, 2, 3, ...
$A_2$	3, 6, ...	$A_2$	1, 3, 4, ...
$F_1$	1, 3, 4, 5, 6, ...	$B_1$	2, 3, 4, ...
$F_2$	2, 3, 4, 5, 6, ...	$B_2$	2, 3, 4, ...
$E$	2, 4, 5, 6, ...	$E$	1, 2, 3, 4, ...

## Symmetries of the elongated box

$\rho$  resonance is in  $I = 1, J^P = 1^-$  channel for pion-pion scattering. Elongated box method tunes the momentum of the scattering particles on the lattice  $\mathbf{p} \propto (\frac{2\pi}{\eta L})$ .



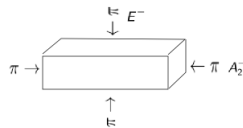
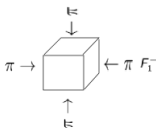
The  $SO(3)$  symmetry group reduce to discrete subgroup  $O_h$  or  $D_{4h}$

$J$	$O_h$	$D_{4h}$
0	$A_1^+$	$A_1^+$
1	$F_1^-$	$A_2^- \oplus E^-$
2	$E^+ \oplus F_2^+$	$A_1^+ \oplus B_1^+ \oplus B_2^+ \oplus E^+$
3	$A_2^- \oplus F_1^- \oplus F_2^-$	$A_2^- \oplus B_1^- \oplus B_2^- \oplus 2E^-$
4	$A_1^+ \oplus E^+ \oplus F_1^+ \oplus F_2^+$	$2A_1^+ \oplus A_2^+ \oplus B_1^+ \oplus B_2^+ \oplus 2E^+$

For the p-wave ( $I = 1$ ) scattering channel, we only need to construct the interpolating fields in  $F_1^-$  in the  $O_h$  group,  $A_2^-$  representations in  $D_{4h}$  group because the energy contribution from angular momenta  $I \geq 3$  is negligible.

# Lüscher's formula for elongated box [1]

Phase shift for  $l = 1$ , rest frame ( $\mathbf{P} = 0$ ):



$$A_2^- : \cot \delta_1(k) = \mathcal{W}_{00} + \frac{2}{\sqrt{5}} \mathcal{W}_{20} \quad (3)$$

(4)

$$\mathcal{W}_{lm}(1, q^2, \eta) = \frac{\mathcal{Z}_{lm}(1, q^2, \eta)}{\eta \pi^{\frac{3}{2}} q^{l+1}}; \quad q = \frac{kL}{2\pi}; \quad \eta = \frac{N_{el}}{N} : \text{elongation factor} \quad (5)$$

Zeta function

$$\mathcal{Z}_{lm}(s; q^2, \eta) = \sum_{\tilde{\mathbf{n}}} \mathcal{Y}_{lm}(\tilde{\mathbf{n}}) (\mathbf{n}^2 - q^2)^{-s}; \quad \mathbf{n} \in \mathbf{m} \quad (6)$$

Total energy

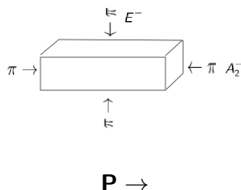
$$E = 2\sqrt{m^2 + k^2}; \quad k = \sqrt{\left(\frac{E}{2}\right)^2 - m^2} \quad (7)$$

[1] X. Feng, X. Li, and C. Liu, Phys.Rev. D70 (2004) 014505



## Lüscher's formula for boost frame

In order to obtain new kinematic region, we boost the resonance along the elongated direction.



$$A_2^- : \cot \delta_1(k) = \mathcal{W}_{00} + \frac{2}{\sqrt{5}} \mathcal{W}_{20} \quad (8)$$

(9)

$$\mathcal{W}_{lm}(1, q^2, \eta) = \frac{\mathcal{Z}_{lm}^{\mathbf{P}}(1, q^2, \eta)}{\gamma \eta \pi^{\frac{3}{2}} q^{l+1}}; \quad \eta = \frac{N_{el}}{N} : \text{elongation factor}; \quad \gamma : \text{boost factor}; \quad (10)$$

$$\mathcal{Z}_{lm}^{\hat{\mathbf{P}}}(s; q^2, \eta) = \sum_{\mathbf{n}} \mathcal{Y}_{lm}(\tilde{\mathbf{n}}) (\tilde{\mathbf{n}}^2 - q^2)^{-s}; \quad \mathbf{n} \in \frac{1}{\gamma} (\mathbf{m} + \frac{\hat{\mathbf{P}}}{2}); \quad (11)$$

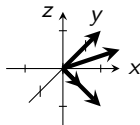
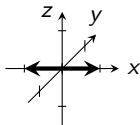
## Interpolating field construction for $\rho$ resonance

Four  $q\bar{q}$  operators and two scattering operators  $\pi\pi$  in  $A_2^-$  sector.

$$\rho^J(t_f) = \bar{u}(t_f)\Gamma_{t_f}A_{t_f}(\mathbf{p})d(t_f); \quad \rho^{J\dagger}(t_i) = \bar{d}(t_i)\Gamma_{t_i}^\dagger A_{t_i}^\dagger(\mathbf{p})u(t_i) \quad (12)$$

$N$	$\Gamma_{t_f}$	$A_{t_f}$	$\Gamma_{t_i}^\dagger$	$A_{t_i}^\dagger$
1	$\gamma_i$	$e^{i\mathbf{p}}$	$-\gamma_i$	$e^{-i\mathbf{p}}$
2	$\gamma_4\gamma_i$	$e^{i\mathbf{p}}$	$\gamma_4\gamma_i$	$e^{-i\mathbf{p}}$
3	$\gamma_i$	$\nabla_j e^{i\mathbf{p}} \nabla_j$	$\gamma_i$	$\nabla_j^\dagger e^{-i\mathbf{p}} \nabla_j^\dagger$
4	$\frac{1}{2}$	$\{e^{i\mathbf{p}}, \nabla_i\}$	$-\frac{1}{2}$	$\{e^{-i\mathbf{p}}, \nabla_i\}$

$$(\pi\pi)_{\mathbf{P},\Lambda,\mu} = \sum_{\mathbf{p}_1^*, \mathbf{p}_2^*} C(\mathbf{P}, \Lambda, \mu; \mathbf{p}_1; \mathbf{p}_2) \pi(\mathbf{p}_1) \pi(\mathbf{p}_2), \quad (13)$$



$$\pi\pi_{100}(\mathbf{p}_1, \mathbf{p}_2, t) = \frac{1}{\sqrt{2}} [\pi^+(\mathbf{p}_1)\pi^-(\mathbf{p}_2) - \pi^+(\mathbf{p}_2)\pi^-(\mathbf{p}_1)]; \quad \mathbf{p}_1 = (1, 0, 0) \quad \mathbf{p}_2 = (-1, 0, 0)$$

$$\pi\pi_{110} = \frac{1}{2} (\pi\pi(110) + \pi\pi(101) + \pi\pi(1-10) + \pi\pi(10-1))$$

## 6 × 6 correlation matrix

$$C = \begin{pmatrix} C_{\rho^J \leftarrow \rho^{J'}} & C_{\rho^J \leftarrow \pi \pi_{100}} & C_{\rho^J \leftarrow \pi \pi_{110}} \\ C_{\pi \pi_{100} \leftarrow \rho^{J'}} & C_{\pi \pi_{100} \leftarrow \pi \pi_{100}} & C_{\pi \pi_{100} \leftarrow \pi \pi_{110}} \\ C_{\pi \pi_{110} \leftarrow \rho^{J'}} & C_{\pi \pi_{110} \leftarrow \pi \pi_{100}} & C_{\pi \pi_{110} \leftarrow \pi \pi_{110}} \end{pmatrix}. \quad (14)$$

The correlation functions:  $\bar{u}(t_i) \longrightarrow u(t_f)$

$$C_{\rho_i \leftarrow \rho_j} = - \left\langle \begin{array}{c} \Gamma_{t_f}^J(\mathbf{p}, t_f) \\ \text{loop} \\ \Gamma_{t_i}^{J'\dagger}(-\mathbf{p}, t_i) \end{array} \right\rangle = - \left\langle \text{Tr}[M^{-1}(t_i, t_f) \Gamma_{t_f}^J e^{i\mathbf{p}} M^{-1}(t_f, t_i) \Gamma_{t_i}^{J'\dagger} e^{-i\mathbf{p}}] \right\rangle. \quad (15)$$

$$C_{\rho_i \leftarrow \pi \pi} = \left\langle \begin{array}{c} \text{triangle} \\ \text{triangle} \end{array} \right\rangle - \left\langle \begin{array}{c} \text{triangle} \\ \text{triangle} \end{array} \right\rangle \stackrel{\mathbf{P}=0}{=} 2 \left\langle \begin{array}{c} \text{triangle} \\ \text{triangle} \end{array} \right\rangle. \quad (16)$$

$$C_{\pi \pi \leftarrow \pi \pi} = - \left\langle \begin{array}{c} \text{square} \\ \text{square} \\ \text{X} \\ \text{X} \\ \text{figure-eight} \\ \text{loop} \end{array} \right\rangle \quad (17)$$

$$\stackrel{\mathbf{P}=0}{=} - \left\langle 2 \begin{array}{c} \text{square} \\ \text{X} \\ \text{figure-eight} \\ \text{loop} \end{array} \right\rangle \quad (18)$$

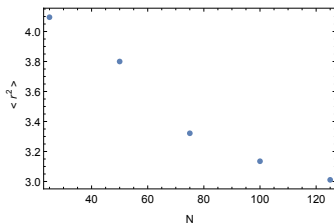
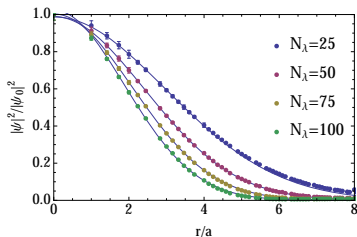
## Laplacian Heaviside smearing [2]

To estimate all-to-all propagators:  
The 3-dimensional gauge-covariant Laplacian operator



$$\tilde{\Delta}^{ab}(x, y; U) = \sum_{k=1}^3 \left\{ \tilde{U}_k^{ab}(x) \delta(y, x + \hat{k}) + \tilde{U}_k^{ba}(y)^* \delta(y, x - \hat{k}) - 2\delta(x, y) \delta^{ab} \right\}. \quad (19)$$

$$S_\Lambda(t) = \sum_{\lambda(t)}^\Lambda |\lambda(t)\rangle \langle \lambda(t)|; \quad \tilde{u}(t) = S(t)u(t) = \sum_{\lambda_t} |\lambda_t\rangle \langle \lambda_t| u(t). \quad (20)$$



[2] C. Morningstar, J. Bulava, J. Foley, K. J. Juge, D. Lenkner, et al., Phys.Rev. D83 (2011) 114505

## Energy spectrum

We implement the calculation in 3 ensembles ( $\eta = 1.0, 1.25, 2.0$ ) at  $m_\pi \approx 310$  MeV and 3 ensembles ( $\eta = 1.0, 1.17, 1.33$ ) at  $m_\pi \approx 227$  MeV with nHYP-smeared clover fermions and two mass-degenerated quark flavor.

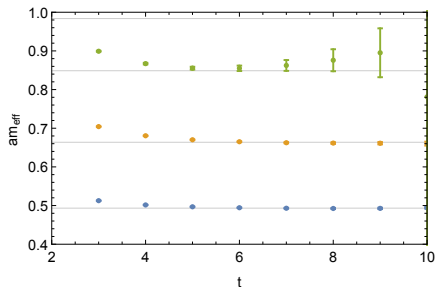
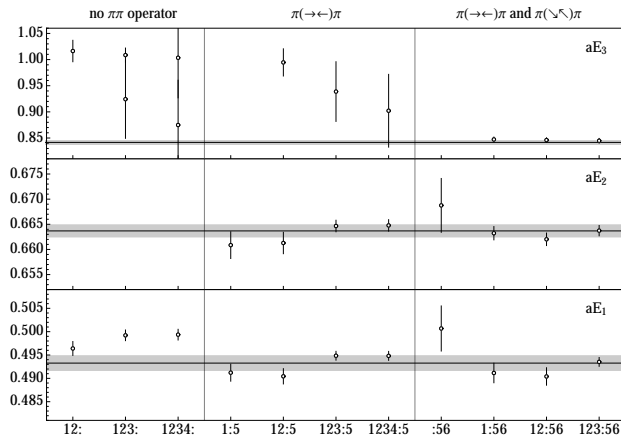


**Figure:** The lowest three energy states with their error bars for  $\eta = 1.0, m_\pi = 310$  MeV ensemble

We extract energy  $E$  by using double exponential  $f(t) = we^{-Et} + (1 - w)e^{-E't}$  to do the  $\chi^2$  fitting for each eigenvalues.

# Energy spectrum



$\mathcal{O}_i$	1	2	3	4	5	6
	$\rho_1$	$\rho_2$	$\rho_3$	$\rho_4$	$\pi\pi_{100}$	$\pi\pi_{110}$

(21)

# Expectation for energy states

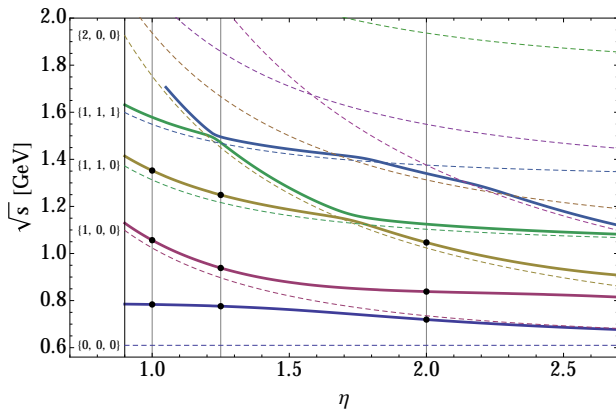
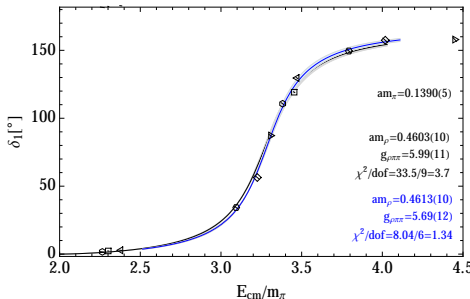
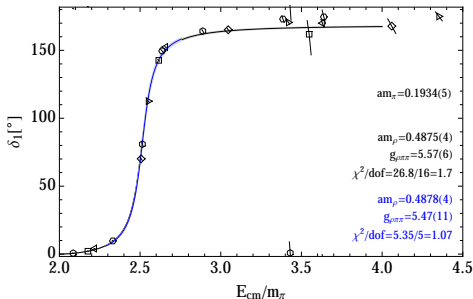


**Figure:** The lowest 3 energy states prediction from  $U\chi PT$  model. When  $\eta = 2.0$  the 3rd state is from operator  $\pi\pi_{200}$  instead of  $\pi\pi_{110}$

# Phase shift fitted with Breit Wigner Form



$$\cot(\delta_1(E)) = \frac{M_R^2 - E^2}{E\Gamma_r(E)}, \quad \Gamma_r(E) \equiv \frac{g_{R12}^2}{6\pi} \frac{p^3}{E^2}. \quad (22)$$

$$\delta_1(E) = \text{arccot} \frac{6\pi(M_R^2 - E^2)E}{g^2 p^3} \quad (23)$$



# Phase shift fitted with $U\chi$ PT model

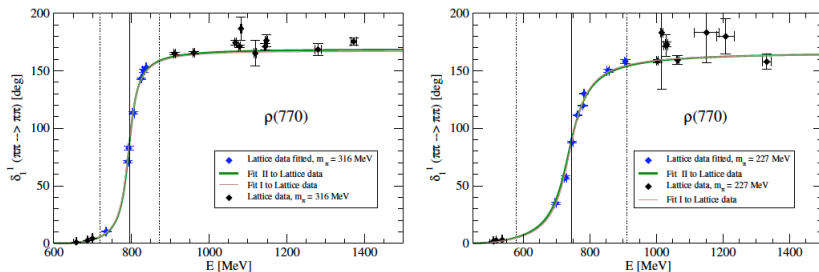
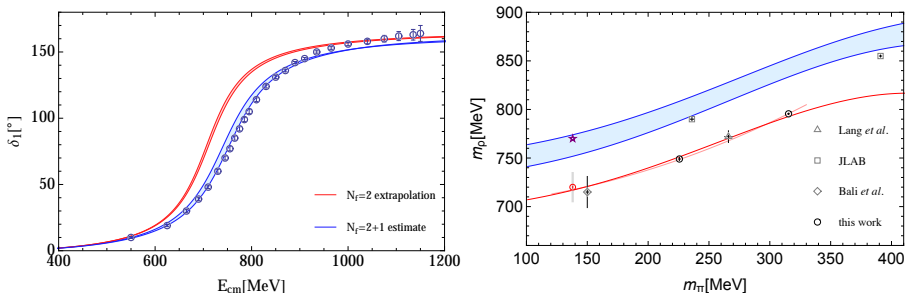


Figure:  $m_\pi \approx 315$  MeV and  $m_\pi \approx 227$  MeV data fitted with  $U\chi$ PT model.

	$m_\pi$	$m_\rho$	$\Gamma_\rho$	$g$	$\chi^2/\text{dof}$
Breit Wigner	315	794.6(6)	37.0(2)	5.57(11)	2.16
$U\chi$ PT		795.2(3)	36.1(1)		1.26
Breit Wigner	227	748.4(1.6)	71.0(8)	5.70(12)	1.46
$U\chi$ PT		748.2(7)	77.0(5)		1.53

## $K\bar{K}$ channel contribution to $\rho$ resonance

We study the  $K\bar{K}$  effect using  $U_\chi$ PT model with input parameters  $m_\pi, f_\pi, f_K$  and low energy constant  $\hat{l}_{1,2}$ .



**Figure:** (Left) Chiral extrapolation of the phase shift to the physical mass (red band), obtained from the simultaneous fit to pion masses. The blue band: phaseshift with  $K\bar{K}$ . Open circles: experiment data [3]

# $m_\rho$ and $g_{\rho\pi\pi}$ comparison

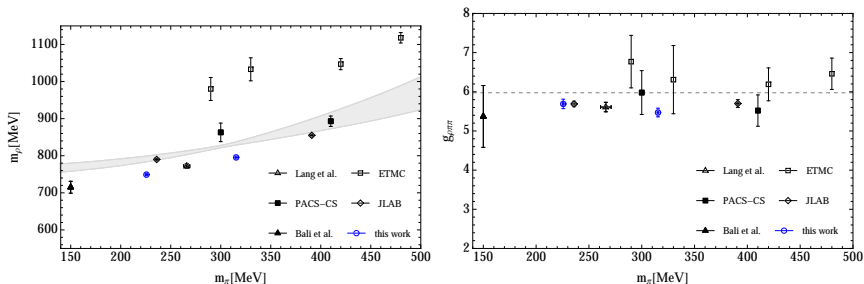


**Figure:** Comparison of different lattice calculation for the  $\rho$  resonance mass (left) and width parameter  $g_{\rho\pi\pi}$  (right). The errors included here are only stochastic. The band in the left plot indicates a  $N_f = 2 + 1$  expectation from  $U_\chi$ PT model constrained by some older lattice QCD data and some other physical input [4].

The results of ETMC are taken from [5]. PACS result is from [6].

# Conclusions

- We complete a precision study of  $\rho$  resonance with LapH smearing method and obtain the resonance parameters at  $m_\pi \approx 310$  MeV and  $m_\pi \approx 227$  MeV.
- For precise energy spectrum results, both Breit Wigner form and  $U\chi PT$  model work well in the resonance region. Modification to the BW is needed when applied to a wider energy region.
- The extrapolation of  $m_\rho$  to physical pion mass is smaller than  $m_\rho^{\text{phy}} = 775$  MeV in a  $N_f = 2$  situation, we believe that this comes from the absence of strange quark and the  $K\bar{K}$  channel which is supported by our  $U\chi PT$  study.



X. Feng, X. Li, and C. Liu, *Two particle states in an asymmetric box and the elastic scattering phases*, *Phys.Rev.* **D70** (2004) 014505, [hep-lat/0404001].



C. Morningstar, J. Bulava, J. Foley, K. J. Juge, D. Lenkner, et al., *Improved stochastic estimation of quark propagation with Laplacian Heaviside smearing in lattice QCD*, *Phys.Rev.* **D83** (2011) 114505, [arXiv:1104.3870].



S. D. Protopopescu, M. Alston-Garnjost, A. Barbaro-Galtieri, S. M. Flatte, J. H. Friedman, T. A. Lasinski, G. R. Lynch, M. S. Rabin, and F. T. Solmitz, *Pi pi Partial Wave Analysis from Reactions  $\pi^+ p \rightarrow \pi^+ \pi^- \Delta^{++}$  and  $\pi^+ p \rightarrow \pi^+ K^- K^+ \Delta^{++}$  at 7.1-GeV/c*, *Phys. Rev.* **D7** (1973) 1279.



J. R. Pelaez and G. Rios, *Chiral extrapolation of light resonances from one and two-loop unitarized Chiral Perturbation Theory versus lattice results*, *Phys. Rev.* **D82** (2010) 114002, [arXiv:1010.6008].



X. Feng, K. Jansen, and D. B. Renner, *Resonance Parameters of the rho-Meson from Lattice QCD*, *Phys.Rev.* **D83** (2011) 094505, [arXiv:1011.5288].



**PACS** Collaboration, S. Aoki et al.,  *$\rho$  Meson Decay in 2+1 Flavor Lattice QCD*, *Phys. Rev.* **D84** (2011) 094505, [arXiv:1106.5365].



P. Estabrooks and A. D. Martin,  *$\pi \pi$  Phase Shift Analysis Below the  $K$  anti- $K$  Threshold*, *Nucl. Phys.* **B79** (1974) 301.

# Symmetries on the lattice

The  $SO(3)$  symmetry group reduce to discrete subgroup  $O_h$  or  $D_{4h}$

**Table:** Resolution of  $2J + 1$  spherical harmonics into the irreducible representations of  $O_h$  and  $D_{4h}$

$J$	$O_h$	$D_{4h}$
0	$A_1^+$	$A_1^+$
1	$F_1^-$	$A_2^- \oplus E^-$
2	$E^+ \oplus F_2^+$	$A_1^+ \oplus B_1^+ \oplus B_2^+ \oplus E^+$
3	$A_2^- \oplus F_1^- \oplus F_2^-$	$A_2^- \oplus B_1^- \oplus B_2^- \oplus 2E^-$
4	$A_1^+ \oplus E^+ \oplus F_1^+ \oplus F_2^+$	$2A_1^+ \oplus A_2^+ \oplus B_1^+ \oplus B_2^+ \oplus 2E^+$

Assume that the energy contribution from angular momenta  $l \geq 3$  is negligible. For example, if we study the p-wave( $l = 1$ ) scattering channel, we should construct the interpolating field in  $F_1^-$  in the  $O_h$  group,  $A_2^-$  and  $E^-$  representations in  $D_{4h}$  group.

## Variational method [?]

Variational method is used to extract energy of the excited states.

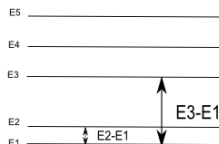
Construct correlation matrix in the interpolator basis

$$C(t)_{ij} = \langle \mathcal{O}_i(t) \mathcal{O}_j^\dagger(0) \rangle; i, j = 1, 2, \dots, \text{number of operators} \quad (24)$$

The eigenvalues of the correlation matrix are

$$\lambda^{(n)}(t, t_0) \propto e^{-E_n t} (1 + \mathcal{O}(e^{-\Delta E_n t})), n = 1, 2, \dots, \text{number of operators} \quad (25)$$

where  $\Delta E_n = E_{\text{Number of operators} + 1} - E_n$ .



Larger energy gap makes the high lying energy decay faster and effective mass plateau appear in an earlier time slice.

## Appendix-B: LapH smearing

Benefit from LapH smearing:

- Keep low frequency mode up to  $\Lambda$  cutoff to compute the all to all propagators,  $u(x) \longrightarrow u(y)$ . The number of propagators  $M^{-1}(t_f, t_i)$  need to be computed reduce from  $6.34 \times 10^{13}$  in position space to  $3.7 \times 10^8$  in momentum space for the  $24^3 48$  ensemble.
- The effective mass reach a plateau in an earlier time slice.

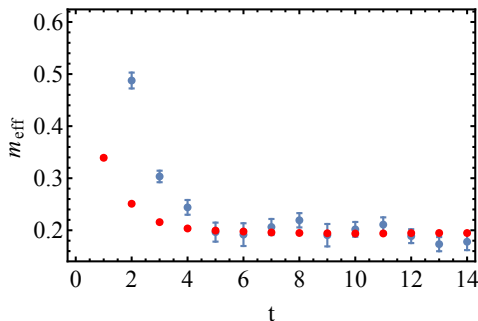


Figure: pion effective mass with (red) and without LapH smearing (blue)



## Appendix-C: Fitting phase-shift

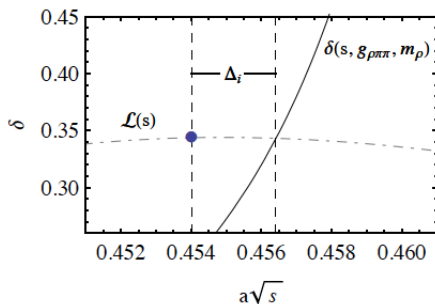


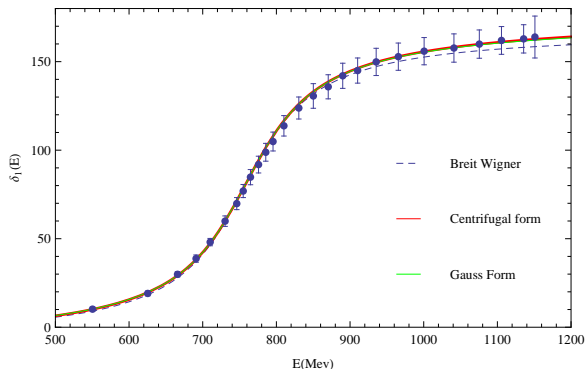
Figure:  $\chi^2$  fitting for the phase shift data to Breit Wigner form

$$\chi^2 = \Delta^T \text{COV}^{-1} \Delta \quad (26)$$

where

$$\Delta_i = \sqrt{s_i^{\text{curve}}} - \sqrt{s_i^{\text{data}}} \quad (27)$$

## Appendix-D: Experiment data [7]



$$\Gamma_{BW}(E) = \frac{g^2}{6\pi} \frac{p^3}{E^2}$$

$$\Gamma_{CF}(E) = \frac{g^2}{6\pi} \frac{p^3}{E^2} \frac{1 + (p_R R)^2}{1 + (p R)^2}$$

$$\Gamma_{GA}(E) = \frac{g^2}{6\pi} \frac{p^3}{E^2} \frac{e^{-p^2/6\beta^2}}{e^{-p_R^2/6\beta^2}}$$

Figure:  $\pi\pi$  phase shift below  $K\bar{K}$  threshold in experiment

[7] Estabrooks, P. and Martin, Alan D. Nucl.Phys. B79 (1974) 301

## K-matrix method

$$T^{-1} = V^{-1} - G = \frac{-3(f^2 - 8l_1 m_\pi^2 + 4l_2 W^2)}{2p^2} - \text{Re}G(W) + \frac{ip}{8\pi W} \quad (28)$$

For K-matrix method the  $\text{Re}G(W) = 0$ .

$$T = \frac{-8\pi W}{p \cot \delta p - ip} \quad (29)$$

$$l_1 = \frac{1}{8\pi^2} \left( -\frac{1}{2} \frac{m_\rho^2}{g_{\rho\pi\pi}^2} + f^2 \right) \quad (30)$$

$$l_2 = -\frac{1}{8g_{\rho\pi\pi}^2} \quad (31)$$